

Energy transfer in two-dimensional magnetohydrodynamic turbulence

Gaurav Dar* and Mahendra K. Verma

Department of Physics

Indian Institute of Technology, Kanpur 208016, India

V. Eswaran

Department of Mechanical Engineering

Indian Institute of Technology, Kanpur 208016, India

In an earlier paper we had developed a method for computing the effective energy transfer between any two Fourier modes in fluid or magnetohydrodynamic (MHD) flows. This method is applied to a pseudo-spectral, direct numerical simulation (DNS) study of energy transfer in the quasi-steady state of 2-D MHD turbulence with large scale kinetic forcing. Two aspects of energy transfer are studied: the energy fluxes, and the energy transfer between different wavenumber regions (*shells*). The picture of energy fluxes that emerges is quite complex — there is a forward cascade of magnetic energy, an inverse cascade of kinetic energy, a flux of energy from the kinetic to the magnetic field, and a reverse flux which transfers the energy back to the kinetic from the magnetic. The energy transfer between different wave number shells is also complex — local and nonlocal transfers often possess opposing features, i.e., energy transfer between some wave number shells occurs from kinetic to magnetic, and between other wave number shells this transfer is reversed. The net transfer of energy is from kinetic to magnetic. The results obtained from the flux studies and the shell-to-shell energy transfer studies are consistent with each other.

arXiv:chao-dyn/9810032v2 14 Jul 2000

*e-mail: gdar@iitk.ac.in

I. INTRODUCTION

In magnetohydrodynamic (MHD) turbulence several scales interact amongst themselves and energy is transferred between them. This transfer plays an important role in the generation of magnetic fields. In this paper we study the energy transfer in two-dimensional(2-D) MHD turbulence. The MHD and Navier Stokes equations show that energy is transferred, in spectral space, to a mode \mathbf{k} from modes \mathbf{p} and \mathbf{q} such that the three wave numbers satisfy the condition $\mathbf{k} + \mathbf{p} + \mathbf{q} = \mathbf{0}$. In an earlier paper (we will refer to this paper as Paper I) [1] we had introduced the idea of *effective* energy transfer between a pair of modes within a triad by the mediation of the third mode, and found the formulae for computing these transfers. In this paper we have applied this method to study energy transfer in 2-D MHD turbulence.

In fluid turbulence the dynamics of energy transfer has been well studied. In 3-D fluid turbulence the kinetic energy is transferred from large scales to small scales, whereas in two dimensions there is an inverse cascade of kinetic energy from small scales to large scales [2]. For MHD turbulence there have been various phenomenological [3–5], analytical [6–13], and numerical studies [14–23] to investigate energy spectra, energy cascade rates, etc. Contrary to fluid turbulence, the direct numerical simulations (DNS) of MHD turbulence show that the *total* energy is transferred from large scales to small scales both in 2-D as well as 3-D turbulence [19,24]. There have been theoretical predictions of the magnitude and directions of only a few of the various fluxes [6,12,8].

Magnetohydrodynamic turbulence is sometimes described in terms of the Elsasser variables $\mathbf{z}^{\pm} = \mathbf{u} \pm \mathbf{b}$. It has been a basic assumption of the phenomenologies for MHD turbulence that the energies associated with \mathbf{z}^{\pm} are transferred to the small scales, and that the flux of the energies is constant in the inertial range in both 2-D and 3-D turbulence [5,25]. Thus the the physics of energy cascades appears to be similar in 2-D and 3-D MHD turbulence.

The magnetic energy of a mode evolves due to two nonlinear terms in the MHD equations— $[\mathbf{b} \cdot (\mathbf{u} \cdot \nabla) \mathbf{b}]$ and $[\mathbf{b} \cdot (\mathbf{b} \cdot \nabla) \mathbf{u}]$ —the first exchanges magnetic energy between different scales, and the second exchanges magnetic and kinetic energy between different scales. The kinetic energy similarly evolves due to two nonlinear terms— $[\mathbf{u} \cdot (\mathbf{u} \cdot \nabla) \mathbf{u}]$ and $[\mathbf{u} \cdot (\mathbf{b} \cdot \nabla) \mathbf{b}]$ —the first one exchanges kinetic energy between different scales and the second exchanges energy between the magnetic and the velocity fields. In this paper we have carried out a detailed investigation of the various energy transfers in 2-D MHD turbulence.

Pouquet *et al.* [8] studied the energy transfer between large and small scales using 3-D EDQNM closure calculations.

They found that the large scales of the magnetic field gain energy in the presence of small-scale residual helicity (which is the difference between kinetic helicity and magnetic helicity). The large scale magnetic field, in turn, was found to enhance the energy exchange between the small-scale magnetic and the velocity fields. This energy exchange resulted in equipartition of small-scale kinetic and magnetic energies. By drawing an analogy between the MHD equation for the magnetic field and the vorticity equation for fluids, Batchelor [26] argued that the transfer between kinetic and magnetic energies takes place primarily at small scales. A similar conjecture was made by Pouquet and Patterson [27]. They also conjectured that an inverse cascade of energy from small-scale to large-scale magnetic field is the mechanism responsible for the enhancement of large-scale magnetic energy. Contrary to the prediction from 3-D EDQNM of Pouquet *et al.* [8], simulations of decaying turbulence by Pouquet and Patterson [27] showed that it is the magnetic helicity and *not* the residual helicity which is important for the growth of large-scale magnetic field.

In a 2-D EDQNM study, Pouquet [6] obtained eddy viscosities for MHD turbulence. She found that the small-scale magnetic energy acts like a negative eddy viscosity on the large-scale magnetic energy. The inverse cascade of the mean-square magnetic vector potential, and hence the enhancement of large-scale magnetic energy, was conjectured to arise due to the destabilization of the of large-scale magnetic field by the small-scale magnetic field. She also found that the small-scale kinetic energy has the effect of a positive eddy viscosity on the large-scale magnetic energy. Ishizawa and Hattori [7] in their EDQNM calculation obtained the eddy viscosity due to each of the nonlinear terms in MHD equations. They found that the eddy viscosity due to $(\mathbf{b} \cdot \nabla) \mathbf{u}$ is positive, leading to a transfer of energy from large-scale magnetic field to small-scale magnetic field. In their calculation, energy was also found to be transferred from the small-scale velocity field to the large-scale magnetic field. Both, Pouquet's [6] and Ishizawa and Hattori's [7] calculations give a non-local energy transfer from small-scale velocity field to the large-scale velocity field.

In a recent work Ishizawa and Hattori [20] employed the wavelet basis to investigate energy transfer in 2-D MHD turbulence. There are some similarities between the observations made by us in this paper and those in the work of Ishizawa and Hattori. Using the formalism developed in Paper I we do a thorough investigation of all the energy transfers. The wavelet basis used by Ishizawa and Hattori [20] is a useful tool for investigating spectral properties and energy transfer properties in different regions of the flow. In Ishizawa's work, the flow was divided into a turbulent and a coherent region which are distinguished by the level of vorticity fluctuations in that region — turbulence is known to have high levels of vorticity fluctuations [28]. They found that the energy transfer between velocity/magnetic scales occurs more efficiently in the turbulent region and less efficiently in the coherent region.

In some of the above mentioned studies [8,27] a distinction was not made between the energies transferred to a mode from the velocity and the magnetic fields. Also, the energy transferred into a mode \mathbf{k} from different wave number regions was not separately computed—only the *net* energy transfer into a wave number \mathbf{k} was obtained. The Eddy damped quasi-normal Markovian (EDQNM) closure calculations dealt mainly with coarse-grained energy transfer (between large scales and small scales). In another study, Frick and Sokoloff [29] solved a shell model of MHD turbulence and calculated only the kinetic energy fluxes between the velocity modes, and the magnetic energy fluxes between the magnetic modes. In our simulations we investigate the (1) various energy fluxes arising within and between the velocity and magnetic fields, and (2) the fine-grained (considering many wave number shells) energy transfer between magnetic and kinetic energies. This gives a more informed picture of the physics of energy transfer in MHD turbulence.

In 3-D MHD turbulent flows, beyond a critical magnetic Reynold number, the magnetic field can grow and reach a steady state [27,30–32]. This is called the *dynamo effect*, and is believed to be the mechanism for the generation of magnetic fields within astrophysical objects. The non-linear transfer in MHD turbulence is important for understanding the growth process of magnetic energy in a dynamo. Although it is not possible to indefinitely maintain a steady state magnetic field in two-dimensional turbulence [33], a steady state can be achieved for a *finite* period of time [6]. This, coupled with the similarity in physics, allows us to probe the non-linear energy transfer in real MHD flows through 2-D simulations. The methods used here are completely generalizable to the 3-D case and can be used to study the dynamo problem directly at a later date.

The paper is organized into the following sections. In Section II we discuss the various energy fluxes and shell-to-shell energy transfer rates which were obtained in Paper I and which we will compute in this paper. The numerical methods used are outlined in Section III. In subsection IIIB, we present a numerical technique to compute the fluxes and the shell-to-shell energy transfer rates. The results are presented in Section IV which is divided into three parts: Subsection IVA outlines the approach used by us to obtain a steady state; Subsections IVB and IVC contain the observations for the energy fluxes and the shell-to-shell energy transfer rates, respectively. The discussion follows in Section V.

II. FORMALISM AND DEFINITIONS

The MHD equations in real space are written as

$$\frac{\partial \mathbf{u}}{\partial t} + (\mathbf{u} \cdot \nabla) \mathbf{u} = -\nabla p + (\mathbf{b} \cdot \nabla) \mathbf{b} + \nu \nabla^2 \mathbf{u}, \quad (1)$$

and

$$\frac{\partial \mathbf{b}}{\partial t} + (\mathbf{u} \cdot \nabla) \mathbf{b} = (\mathbf{b} \cdot \nabla) \mathbf{u} + \mu \nabla^2 \mathbf{b} \quad (2)$$

where \mathbf{u} and \mathbf{b} are the velocity and magnetic fields respectively, and ν and μ are the fluid kinematic viscosity and magnetic diffusivity respectively. In Fourier space, the kinetic energy and magnetic energy evolution equations for a Fourier mode are

$$\frac{\partial E^u(\mathbf{k})}{\partial t} + 2\nu k^2 E^u(\mathbf{k}) = \sum_{\mathbf{k}+\mathbf{p}+\mathbf{q}=0} \frac{1}{2} S^{uu}(\mathbf{k}|\mathbf{p}, \mathbf{q}) + \sum_{\mathbf{k}+\mathbf{p}+\mathbf{q}=0} \frac{1}{2} S^{ub}(\mathbf{k}|\mathbf{p}, \mathbf{q}) \quad (3)$$

$$\frac{\partial E^b(\mathbf{k})}{\partial t} + 2\mu k^2 E^b(\mathbf{k}) = \sum_{\mathbf{k}+\mathbf{p}+\mathbf{q}=0} \frac{1}{2} S^{bb}(\mathbf{k}|\mathbf{p}, \mathbf{q}) + \sum_{\mathbf{k}+\mathbf{p}+\mathbf{q}=0} \frac{1}{2} S^{bu}(\mathbf{k}|\mathbf{p}, \mathbf{q}) \quad (4)$$

where $E^u(\mathbf{k}) = |\mathbf{u}(\mathbf{k})|^2/2$ is the kinetic energy, and $E^b(\mathbf{k}) = |\mathbf{b}(\mathbf{k})|^2/2$ is the magnetic energy. The four nonlinear terms $S^{uu}(\mathbf{k}|\mathbf{p}, \mathbf{q})$, $S^{ub}(\mathbf{k}|\mathbf{p}, \mathbf{q})$, $S^{bb}(\mathbf{k}|\mathbf{p}, \mathbf{q})$ and $S^{bu}(\mathbf{k}|\mathbf{p}, \mathbf{q})$ are

$$S^{uu}(\mathbf{k}|\mathbf{p}, \mathbf{q}) = -Re(i[\mathbf{k} \cdot \mathbf{u}(\mathbf{q})][\mathbf{u}(\mathbf{k}) \cdot \mathbf{u}(\mathbf{p})] + i[\mathbf{k} \cdot \mathbf{u}(\mathbf{p})][\mathbf{u}(\mathbf{k}) \cdot \mathbf{u}(\mathbf{q})]) \quad (5)$$

$$S^{bb}(\mathbf{k}|\mathbf{p}, \mathbf{q}) = -Re(i[\mathbf{k} \cdot \mathbf{u}(\mathbf{q})][\mathbf{b}(\mathbf{k}) \cdot \mathbf{b}(\mathbf{p})] + i[\mathbf{k} \cdot \mathbf{u}(\mathbf{p})][\mathbf{b}(\mathbf{k}) \cdot \mathbf{b}(\mathbf{q})]) \quad (6)$$

$$S^{ub}(\mathbf{k}|\mathbf{p}, \mathbf{q}) = Re(i[\mathbf{k} \cdot \mathbf{b}(\mathbf{q})][\mathbf{u}(\mathbf{k}) \cdot \mathbf{b}(\mathbf{p})] + i[\mathbf{k} \cdot \mathbf{b}(\mathbf{p})][\mathbf{u}(\mathbf{k}) \cdot \mathbf{b}(\mathbf{q})]) \quad (7)$$

$$S^{bu}(\mathbf{k}|\mathbf{p}, \mathbf{q}) = Re(i[\mathbf{k} \cdot \mathbf{b}(\mathbf{q})][\mathbf{b}(\mathbf{k}) \cdot \mathbf{u}(\mathbf{p})] + i[\mathbf{k} \cdot \mathbf{b}(\mathbf{p})][\mathbf{b}(\mathbf{k}) \cdot \mathbf{u}(\mathbf{q})]) \quad (8)$$

These terms are conventionally taken to represent the nonlinear transfer from modes \mathbf{p} and \mathbf{q} to mode \mathbf{k} [2,34]. Note that the wavenumber triad \mathbf{k} , \mathbf{p} and \mathbf{q} should satisfy the condition $\mathbf{k} + \mathbf{p} + \mathbf{q} = 0$. The term $S^{uu}(\mathbf{k}|\mathbf{p}, \mathbf{q})$ represents

the net transfer of kinetic energy from modes \mathbf{p} and \mathbf{q} to mode \mathbf{k} . Likewise the term $S^{ub}(\mathbf{k}|\mathbf{p}, \mathbf{q})$ is the net magnetic energy transferred from modes \mathbf{p} and \mathbf{q} to the kinetic energy in mode \mathbf{k} , whereas $S^{bu}(\mathbf{k}|\mathbf{p}, \mathbf{q})$ is the net kinetic energy transferred from modes \mathbf{p} and \mathbf{q} to the magnetic energy in mode \mathbf{k} . The term $S^{bb}(\mathbf{k}|\mathbf{p}, \mathbf{q})$ represents the transfer of magnetic energy from modes \mathbf{p} and \mathbf{q} to mode \mathbf{k} . Thus, the quantities $S^{uu}(\mathbf{k}|\mathbf{p}, \mathbf{q})$, $S^{ub}(\mathbf{k}|\mathbf{p}, \mathbf{q})$, $S^{bb}(\mathbf{k}|\mathbf{p}, \mathbf{q})$, and $S^{bu}(\mathbf{k}|\mathbf{p}, \mathbf{q})$ represent the nonlinear energy transfer from the *two modes* \mathbf{p} and \mathbf{q} to mode \mathbf{k} . We define the following quantities :

$$\mathcal{S}^{uu}(\mathbf{k}|\mathbf{p}|\mathbf{q}) = -Re (i[\mathbf{k} \cdot \mathbf{u}(\mathbf{q})][\mathbf{u}(\mathbf{k}) \cdot \mathbf{u}(\mathbf{p})]), \quad (9)$$

$$\mathcal{S}^{bb}(\mathbf{k}|\mathbf{p}|\mathbf{q}) = -Re (i[\mathbf{k} \cdot \mathbf{u}(\mathbf{q})][\mathbf{b}(\mathbf{k}) \cdot \mathbf{b}(\mathbf{p})]), \quad (10)$$

$$\mathcal{S}^{ub}(\mathbf{k}|\mathbf{p}|\mathbf{q}) = Re (i[\mathbf{k} \cdot \mathbf{b}(\mathbf{q})][\mathbf{u}(\mathbf{k}) \cdot \mathbf{b}(\mathbf{p})]), \quad (11)$$

$$\mathcal{S}^{bu}(\mathbf{k}|\mathbf{p}|\mathbf{q}) = Re (i[\mathbf{k} \cdot \mathbf{b}(\mathbf{q})][\mathbf{b}(\mathbf{k}) \cdot \mathbf{u}(\mathbf{p})]). \quad (12)$$

. where Eqs. (9)-(12) are the first terms on the right hand side of Eqs. (5)-(8). In Paper I, we showed that the the expressions in Eqs. (9)-(12) have the following interpretation : $\mathcal{S}^{uu}(\mathbf{k}|\mathbf{p}|\mathbf{q})$ is the kinetic energy *effectively* transferred from mode \mathbf{p} to mode \mathbf{k} ; $\mathcal{S}^{bb}(\mathbf{k}|\mathbf{p}|\mathbf{q})$ is the magnetic energy effectively transferred from mode \mathbf{p} to mode \mathbf{k} ; $\mathcal{S}^{ub}(\mathbf{k}|\mathbf{p}|\mathbf{q})$ is the magnetic energy effectively transferred from mode \mathbf{p} to kinetic energy in mode \mathbf{k} , and $\mathcal{S}^{bu}(\mathbf{k}|\mathbf{p}|\mathbf{q})$ is the kinetic energy effectively transferred from mode \mathbf{p} to magnetic energy in mode \mathbf{k} . In all these effective energy transfers the mode with wavenumber \mathbf{q} *mediates* the transfer but does not itself gain or lose *net* energy. We discussed in Paper I that Eqs. (9)-(12) give us a method of computing energy exchange between any two modes. This method allows us to have a much better understanding of cascade rates between scales.

In this paper, we use the term *u*-sphere (*b*-sphere) to represent a sphere in wavenumber space enclosing velocity (magnetic) modes. Thus the energy associated with a *u*-sphere (*b*-sphere) is kinetic (magnetic) energy. In Paper I, the idea of effective mode-to-mode transfer rate was used to define the following energy fluxes and shell-to-shell energy transfer rates. The flux $\Pi_{b <}^{u <}(K)$ is the kinetic energy lost by a *u*-sphere of radius K to the magnetic energy of the *b*-sphere of the same radius, i.e.,

$$\Pi_{b <}^{u <}(K) = \sum_{|\mathbf{k}| < K} \sum_{|\mathbf{p}| < K} \mathcal{S}^{bu}(\mathbf{k}|\mathbf{p}|\mathbf{q}); \quad (13)$$

where the summation is restricted such that $\mathbf{k} + \mathbf{p} + \mathbf{q} = \mathbf{0}$. The flux $\Pi_{b>}^{u<}(K)$ is the energy lost by a u -sphere to modes outside the corresponding b -sphere, i.e.,

$$\Pi_{b>}^{u<}(K) = \sum_{|\mathbf{k}|>K} \sum_{|\mathbf{p}|<K} \mathcal{F}^{bu}(\mathbf{k}|\mathbf{p}|\mathbf{q}); \quad (14)$$

The flux $\Pi_{u>}^{b<}(K)$ is the energy lost by a b -sphere to modes outside the u -sphere, i.e.,

$$\Pi_{u>}^{b<}(K) = \sum_{|\mathbf{k}|>K} \sum_{|\mathbf{p}|<K} \mathcal{F}^{ub}(\mathbf{k}|\mathbf{p}|\mathbf{q}). \quad (15)$$

The flux $\Pi_{b>}^{u>}(K)$ is the energy lost by modes outside a u -sphere to those outside the corresponding b -sphere, i.e.,

$$\Pi_{b>}^{u>}(K) = \sum_{|\mathbf{k}|>K} \sum_{|\mathbf{p}|>K} \mathcal{F}^{bu}(\mathbf{k}|\mathbf{p}|\mathbf{q}). \quad (16)$$

These are the only fluxes from u to b modes. The fluxes for the kinetic-to-kinetic and magnetic-to-magnetic energy transfers can also be written in terms of the mode-to-mode transfers \mathcal{F}^{uu} and \mathcal{F}^{bb} respectively. Flux $\Pi_{u>}^{u<}(K)$ is the energy lost by u -sphere to modes outside the u -sphere, i.e.,

$$\Pi_{u>}^{u<}(K) = \sum_{|\mathbf{k}|>K} \sum_{|\mathbf{p}|<K} \mathcal{F}^{uu}(\mathbf{k}|\mathbf{p}|\mathbf{q}). \quad (17)$$

Similarly, the flux $\Pi_{b>}^{b<}(K)$ is the energy lost by a b -sphere to modes outside the b -sphere, i.e.,

$$\Pi_{b>}^{b<}(K) = \sum_{|\mathbf{k}|>K} \sum_{|\mathbf{p}|<K} \mathcal{F}^{bb}(\mathbf{k}|\mathbf{p}|\mathbf{q}). \quad (18)$$

The total flux is defined as the total energy (kinetic+magnetic) lost by the K -sphere to the modes outside, i.e.,

$$\Pi_{tot}(K) = \Pi_{u>}^{u<}(K) + \Pi_{b>}^{b<}(K) + \Pi_{b>}^{u>}(K) + \Pi_{u>}^{b<}(K). \quad (19)$$

Similarly, from Paper I, the *shell-to-shell* energy transfer rate from the n^{th} u -shell to the m^{th} b -shell is given by

$$T_{mn}^{bu} = \sum_{\mathbf{k} \in m} \sum_{\mathbf{p} \in n} \mathcal{F}^{bu}(\mathbf{k}|\mathbf{p}|\mathbf{q}). \quad (20)$$

The shell-to-shell energy transfer rate from the n^{th} u -shell to the m^{th} u -shell is given by

$$T_{mn}^{uu} = \sum_{\mathbf{k} \in m} \sum_{\mathbf{p} \in n} \mathcal{F}^{uu}(\mathbf{k}|\mathbf{p}|\mathbf{q}). \quad (21)$$

The shell-to-shell energy transfer rate from the n^{th} b -shell to the m^{th} b -shell is given by

$$T_{mn}^{bb} = \sum_{\mathbf{k} \in m} \sum_{\mathbf{p} \in n} \mathcal{F}^{bb}(\mathbf{k}|\mathbf{p}|\mathbf{q}). \quad (22)$$

The energy transfer rate from the m^{th} b -shell to the n^{th} u -shell, $T_{nm}^{ub} = -T_{mn}^{bu}$.

In this paper, we have performed a direct numerical simulation of MHD turbulence and using the values of Fourier modes obtained in the simulation, we have calculated various fluxes [Eqs. (13)-(18)] and energy transfer rates [Eqs. (20)-(22)]. The details of the numerical methods used to compute these quantities and to solve the MHD equations are presented in the following section.

III. SIMULATION DETAILS

A. Numerical Method

In our simulations we use the Elsässer variable $\mathbf{z}^\pm = \mathbf{u} \pm \mathbf{b}$ instead of \mathbf{u} and \mathbf{b} . The MHD equations (1) and (2) written in terms of \mathbf{z}^+ and \mathbf{z}^- are

$$\begin{aligned} \frac{\partial \mathbf{z}^\pm}{\partial t} \mp (\mathbf{B}_0 \cdot \nabla) \mathbf{z}^\pm + (\mathbf{z}^\mp \cdot \nabla) \mathbf{z}^\pm = & -\nabla p + \nu_\pm \nabla^2 \mathbf{z}^\pm + \nu_\mp \nabla^2 \mathbf{z}^\mp \\ & + (\nu_\pm/k_{eq}^2) \nabla^4 \mathbf{z}^\pm + (\nu_\mp/k_{eq}^2) \nabla^4 \mathbf{z}^\mp + \mathbf{F}^\pm \end{aligned} \quad (23)$$

where $\nu^\pm = (\nu \pm \mu)/2$. In addition to the viscosity and the magnetic diffusivity in Eqs.(1) and (2), the Eq. (23) includes hyperviscosity (ν^\pm/k_{eq}^2) to damp out the energy at very high wave numbers. We choose $\nu = \mu = 5 \times 10^{-6}$ for runs on a grid of size 512×512 . The parameter k_{eq} is chosen to be 14 in all the runs. The terms \mathbf{F}^\pm are the forcing functions. The corresponding forcing functions for the \mathbf{u} and the \mathbf{b} fields are related to \mathbf{F}^\pm , i.e., $\mathbf{F}^u = (\mathbf{F}^+ + \mathbf{F}^-)/2$ and $\mathbf{F}^b = (\mathbf{F}^+ - \mathbf{F}^-)/2$ respectively. In our simulations, we do not force the magnetic field (i.e, $\mathbf{F}^b = 0$). Consequently, we get $\mathbf{F}^+ = \mathbf{F}^- = \mathbf{F}^u = \mathbf{F}$.

We use the pseudo-spectral method [35] to solve the above equations in a periodic box of size $2\pi \times 2\pi$. In order to remove the aliasing errors arising in the pseudo-spectral method a square truncation is performed wherein all the modes with $|k_x| \geq N/3$ or $|k_y| \geq N/3$ are set equal to zero. The equations are time advanced using the second order Adam-Bashforth scheme for the convective term and the Crank-Nicholson scheme for the viscous terms. The time step Δt used for these runs is 5×10^{-4} . All the quantities are non-dimensionalised using the initial total energy and length scale of 2π . For the simulation results shown in this paper $\sigma_c \approx 0.1$. However, we have carried out simulations upto $\sigma_c \approx 0.9$ and the results obtained for higher σ_c 's were found to be qualitatively similar to those shown in this paper.

At each time step we construct \mathbf{F} as an uncorrelated random function that is divergence free (i.e., $\nabla \cdot \mathbf{F} = 0$). The x -component of \mathbf{F} is determined at every time step by

$$F_x = \left(\frac{k_y}{k}\right) \sqrt{\Delta t} \mathcal{F} e^{i\phi}, \quad (24)$$

where \mathcal{F}^2 is equal to the average energy input rate per mode, and phase ϕ is a uniformly distributed random variable between 0 and 2π . The y -component of the forcing function is obtained by using the condition of zero divergence, i.e.,

$$F_y = -\left(\frac{k_x}{k}\right) \sqrt{\Delta t} \mathcal{F} e^{i\phi}, \quad (25)$$

We implement the forcing over a k -space annulus $4 < k < 5$. The value of \mathcal{F}^2 is determined from the average rate of the total energy input which is chosen to be equal to 0.1.

B. Numerical computation of fluxes

To compute the fluxes we employ a method similar to that used by Domaradzki and Rogallo [36]. We outline this method below using $\Pi_{u^>}^{b^<}(K)$ as an example. In Eq. (15) we substitute the expression for $S^{ub}(\mathbf{k}|\mathbf{p}|\mathbf{q})$ [Eq. (11)] :

$$\Pi_{u^>}^{b^<}(K) = \sum_{|\mathbf{k}|>K} \sum_{|\mathbf{p}|<K} Re(i[\mathbf{k} \cdot \mathbf{b}(\mathbf{q})][\mathbf{u}(\mathbf{k}) \cdot \mathbf{b}(\mathbf{p})]) \quad (26)$$

A straightforward summation over \mathbf{k} and \mathbf{p} involves $O(N^2)$ operations, where N is the size of the grid, and would thus involve a prohibitive computational cost for high N (i.e., high Reynolds number) simulations. Instead, the pseudo-spectral method can be used to compute Eq. (26) in $O(N \log N)$ operations. It involves the following procedure.

We define two ‘truncated’ variables $\mathbf{u}^>$ and $\mathbf{b}^<$ as follows

$$\mathbf{u}^>(\mathbf{k}) = \begin{cases} 0 & \text{if } |\mathbf{k}| < K \\ \mathbf{u}(\mathbf{k}) & \text{if } |\mathbf{k}| > K \end{cases} \quad (27)$$

and

$$\mathbf{b}^<(\mathbf{p}) = \begin{cases} \mathbf{b}(\mathbf{p}) & \text{if } |\mathbf{p}| < K \\ 0 & \text{if } |\mathbf{p}| > K \end{cases} \quad (28)$$

The Eq. (26) written in terms of $\mathbf{u}^>$ and $\mathbf{b}^<$ reads as follows

$$\Pi_{u^>}^{b^<}(K) = \sum_{\mathbf{k}} \sum_{\mathbf{p}} Re(i[\mathbf{k} \cdot \mathbf{b}(\mathbf{k} - \mathbf{p})][\mathbf{u}^>(\mathbf{k}) \cdot \mathbf{b}^<(\mathbf{p})]). \quad (29)$$

The above equation may be written as

$$\Pi_{u^>}^{b^<}(K) = Re \left[\sum_{\mathbf{k}} ik_j u_i^>(\mathbf{k}) \sum_{\mathbf{p}} b_j(\mathbf{k} - \mathbf{p}) b_i^<(\mathbf{p}) \right] \quad (30)$$

The \mathbf{p} summation in the equation above can be recognized as a convolution sum. The right hand side of Eq. (30) can be conveniently and efficiently evaluated by the pseudo-spectral method, using the truncated variables $\mathbf{u}^>$ and $\mathbf{b}^<$. This procedure has to be repeated for every value of K for which the flux needs to be computed. The rest of the fluxes defined in Eqs. (13)-(18) and also the transfer rates defined in Eqs. (20)-(22) are similarly computed.

In the following section we describe the results of our simulations.

IV. RESULTS

A. Generation of Steady State

The computational time required to obtain a statistically steady state on a grid of size 512^2 is large. So to obtain a steady state in simulations on this grid we proceed in stages. We run on a grid of size 64^2 till a steady state is achieved. This steady state field is then used as the initial condition to achieve a steady state in a simulation on a grid of size 128^2 and so on to grids 256^2 and then 512^2 .

It is theoretically expected that in 2-D, in the long term, the magnetic energy *will* decay [33] even if kinetic energy is stationary. In our simulations we found that the fields remain steady for the period over which the simulation was performed (Fig. 1). Since the $N = 512^2$ simulations are computationally expensive, we have instead shown the decay of magnetic energy for a $N = 128^2$ simulation. The magnetic energy is found to have a quasi-steady state over the time interval extending from approximately $t = 20 - - - 30$ and it decays over the remaining period, as is theoretically expected. For the $N = 512^2$ simulation too, after the period of stationarity, the simulations should show decay of magnetic energy. So, strictly speaking, our steady state is only a quasi-steady state. In Fig. 1 we show the magnetic and kinetic energy in a quasi-steady state. The Alfvén ratio (the ratio of kinetic to magnetic energy) is found to fluctuate between the values 0.4 and 0.56. Hence over the steady state magnetic energy dominates over the kinetic energy. We compute the fluxes and the shell-to-shell transfer rates over this quasi-steady state once in every unit of non-dimensional time. The fluxes and transfer rates are shown in this paper after averaging over 15 time units in quasi-steady state.

B. Flux studies

In our numerical simulations we have computed all the energy fluxes defined in Eqs. (13)-(18). In this section we discuss these energy fluxes (cascade rates).

In Fig. 2 we show all the fluxes. The total flux Π_{tot} is positive indicating that there is a net loss of energy from the K -sphere to modes outside for all K . In the wavenumber region $25 < K < 50$, the total flux is seen to be approximately constant. This wave number region is the inertial range.

The net transfer from kinetic to magnetic energy is a sum of the fluxes $\Pi_{b<}^{u<}(K)$, $\Pi_{b>}^{u<}(K)$, $\Pi_{b<}^{u>} [= -\Pi_{u>}^{b<}(K)]$, and $\Pi_{b>}^{u>}(K)$. In our 512^2 simulations, the sphere of radius $K_{max} = 241$ encloses all the modes. We observe from Fig. 2 that the fluxes $\Pi_{b>}^{u<}(K_{max})$, $\Pi_{b<}^{u>}(K_{max})$ and $\Pi_{b>}^{u>}(K_{max})$ are zero, as there are no modes outside this sphere of maximum radius K_{max} . The flux $\Pi_{b<}^{u<}(K_{max})$ is found to be positive (see Fig. 2), indicating that there is a net transfer from kinetic energy to magnetic energy; since the magnetic modes are not being forced, it is this transfer that keeps the magnetic energy constant in quasi-steady state.

We now describe features of the fluxes $\Pi_{b<}^{u<}$, $\Pi_{b>}^{u<}$, $\Pi_{u>}^{b<}$, $\Pi_{b>}^{u>}$, $\Pi_{u>}^{b<}$, and $\Pi_{b<}^{u>}$ observed in our simulations and plotted in Fig. 2. We remind the reader that the u -modes within a wave number sphere are called the u -sphere and the b -modes within the wave number sphere are called the b -sphere. First, we discuss the fluxes that transfer energy between the u -modes and the b -modes. We find that the flux $\Pi_{b<}^{u<}(K)$ is positive — hence, kinetic energy is lost by a u -sphere to the corresponding b -sphere. The flux $\Pi_{b>}^{u<}(K)$ is also positive. It means that a u -sphere loses energy to the modes outside the b -sphere. We find that the flux $\Pi_{u>}^{b<}(K)$ is negative, which implies that the b -sphere gains energy from modes outside the u -sphere. Thus, all these fluxes result in a transfer of kinetic energy to magnetic energy. However, $\Pi_{b>}^{u>}(K)$ is negative, implying that there is some feedback of energy from modes outside the b -sphere to modes outside the u -sphere. The *net* transfer, however, is from kinetic to magnetic. We shall later show that the flux $\Pi_{b>}^{u>}(K)$ plays a crucial role in driving the kinetic-to-kinetic flux $\Pi_{u>}^{u<}(K)$.

The energy gained by the b -spheres is found to be constant for the approximate range $20 \leq K \leq K_{max}$. This can be seen from the plot of $\Pi_{u<}^{b<}(K) + \Pi_{u>}^{b<}$ (which is the negative of the total transfer of kinetic energy to the modes within the b -sphere). The constancy of the flux implies that a b -sphere of radius K and that of radius of $K + \Delta K$ get the same amount of energy from the u -modes. Thus there is no *net* energy transfer from the u -modes into a b -shell (of thickness ΔK) beyond approximately $K = 20$. We therefore conclude that the *net* energy transfer from u -modes

to the b -sphere occurs within the $K \leq 20$ sphere.

We find that there is a kinetic energy gain by the u -sphere from u -modes outside due to the fact that flux $\Pi_u^{u \leq}(K)$ is negative — this is consistent with the numerical simulations of Ishizawa and Hattori [20]. This behaviour of kinetic energy is known as an ‘inverse cascade’ in literature and is reminiscent of the inverse cascade of kinetic energy in 2-D fluid turbulence [2] and of mean square vector potential in 2-D MHD turbulence [6,37]. Note, however that the kinetic energy in 2-D MHD turbulence is not an inviscid invariant. Fig. 2 shows that the inverse cascade of kinetic energy exists in the wave number range $K \leq 60$. Even the modes that are being forced ($4 \leq k \leq 5$) gain energy from higher wave numbers u -modes. The source of this energy is the flux $\Pi_u^{b >}(K) [= -\Pi_b^{u >}(K)]$ which transfers energy from higher b -modes to the higher u -modes and thus effectively forces them.

We observe from Fig. 2 that there is a loss of magnetic energy from the b -sphere to the b -modes outside [see $\Pi_b^{b \leq}(K)$], i.e., a forward cascade of magnetic energy — this was also observed in the numerical simulations of Ishizawa and Hattori [20]. Our observation of a forward cascade of magnetic energy contradicts the result of the EDQNM closure calculations which predicts an inverse cascade of magnetic energy [6].

The flux $\Pi_b^{b \leq}(K)$ is found to be constant in the inertial range. Using similar reasoning to that given above, we can conclude that the net magnetic energy transfer to a wave number shell in the inertial range is zero. However, in this case it would imply that the *entire* energy gained by the shell (of thickness ΔK) from the b -sphere of radius K is lost *completely* to the modes outside the region $K + \Delta K$. Thus the magnetic energy cascades down to higher wave numbers independently of the transfers between kinetic and magnetic energy in the inertial range, which are quite significant (see below). This flux of magnetic energy is sustained by the fluxes $\Pi_b^{u \leq}(K)$ and $\Pi_b^{u >}(K)$, both of which transfer kinetic energy into the small b -spheres.

Figure 3 schematically illustrates the energy fluxes of Fig. 2 for a K sphere of radius $K = 20$, which is within the inertial range. The energy input due to forcing and the small inverse cascade [$\Pi_u^{u \leq}(K)$] into the u -sphere from higher u -modes, provides the energy input into the u -sphere. This energy is transferred into and outside the b -sphere by $\Pi_b^{u \leq}(K)$ and $\Pi_b^{u >}(K)$, the latter transfer being the most significant of all transfers (see Figs. 2 and 3). The energy transferred into the b -sphere from the u -sphere [$\Pi_b^{u \leq}(K)$], and a negligible input from the modes outside the u -sphere [$-\Pi_u^{b \leq}(K)$], cascades down to the higher wave number b -modes. In the higher b -modes, this cascaded energy [$\Pi_b^{b \leq}(K)$], together with the transfer from the u -sphere, is partly dissipated and partly fed back to the high wave number u -modes. This feedback to the kinetic energy is mostly dissipated, though a small inverse cascade takes some

energy back into the u -sphere. This is the qualitative picture of the energy transfer in 2-D MHD turbulence.

The net transfer to each of the four corners of the Fig. 3 sum to zero within the statistical error (which is computed from the standard deviation of the sampled data). This is consistent with a quasi-steady-state picture.

The results presented here for the quasi-steady-state in a forced turbulence remain qualitatively valid even for a decaying case — the direction of the various fluxes for the decaying case are identical to that for the forced simulation; but as the energy decays, the magnitudes of all the fluxes reduce.

The fluxes give us information about the overall energy transfer from a wave number sphere or outside-sphere to another sphere or outside-sphere. To obtain a more detailed account of the energy transfer, energy exchange between the wave number shells are now studied. In the following section we present a discussion on the shell-to-shell energy transfer rates in MHD turbulence.

C. Shell-to-Shell energy transfer-rate studies

Significant details of energy transfers are revealed by calculating the shell-to-shell energy transfer rates T_{mn}^{uu} , T_{mn}^{bb} , T_{mn}^{bu} defined in Eqs. (21)-(20). We partition the k -space into shells at wave numbers $k_n (n = 1, 2, 3, \dots) = 1, 16, 19.02, 22.62, \dots, 2^{(n+14)/4}$. The first shell extends from $k_1 = 1$ to $k_2 = 16$ — a division of the wave number space into smaller shells at these lower wavenumbers will contain too few modes; the second shell extends from $k_2 = 16$ to $k_3 = 19.02$, ..., the m^{th} shell extends from k_m to $k_{(m+1)}$. Thus, the effective shell-to-shell energy transfer rate from the n^{th} u -shell to the m^{th} u -shell [Eq. (21)] can be written as,

$$T_{mn}^{uu} = \sum_{k_m < k < k_{m+1}} \sum_{k_n < p < k_{n+1}} \sum_{\mathbf{q}}^{\Delta} \mathcal{F}^{uu}(\mathbf{k}|\mathbf{p}|\mathbf{q}), \quad (31)$$

and the effective shell-to-shell energy transfer rate from the n^{th} b -shell to the m^{th} b -shell [Eq. (22)] can be written as

$$T_{mn}^{bb} = \sum_{k_m < k < k_{m+1}} \sum_{k_n < p < k_{n+1}} \sum_{\mathbf{q}}^{\Delta} \mathcal{F}^{bb}(\mathbf{k}|\mathbf{p}|\mathbf{q}). \quad (32)$$

and the effective shell-to-shell energy transfer rate from the n^{th} u -shell to the m^{th} b -shell, as defined in Eq. (20) can be written as,

$$T_{mn}^{bu} = \sum_{k_m < k < k_{m+1}} \sum_{k_n < p < k_{n+1}} \sum_{\mathbf{q}}^{\Delta} \mathcal{F}^{bu}(\mathbf{k}|\mathbf{p}|\mathbf{q}). \quad (33)$$

We categorise the energy transfer between u -shells and the b -shells as being *homologous* if the transfers are between the corresponding shells (of the same wave number range $k_n < k < k_{n+1}$, say). Transfers between different shells

are therefore *non-homologous*. Further, transfers (kinetic-to-magnetic, kinetic-to-kinetic, and magnetic-to-magnetic) involving shells which are close in wave number space are called *local* transfers, as is the convention. Two shells are considered close if the wave number ratio of the larger shell to the smaller shell is less than 2 (in this study this would include the shells between $n + 4$ to $n - 4$ from the n^{th} shell). Transfers involving shells more distant are called *non-local*.

In Fig. 4 we plot the energy transfer rates T_{mn}^{bu} between u -shells and b -shells. It is evident from the figure that the transfer rates between shells in the inertial range are virtually independent of the individual values of the indices m and n , and only dependent on their differences. This means that the transfer rates in the inertial range are *self-similar*. The differences in T_{mn}^{bu} for various n are smaller than the standard deviation of the sampled data, indicating that the perceived self-similarity is statistically significant.

We now discuss our simulation results for the non-homologous transfer rates between u -shells and b -shells. In Fig. 4 we have shown these transfer rates from the n^{th} u -shell to the m^{th} b -shell by plotting T_{mn}^{bu} versus m for various values of n . We find that for all m , except for $m = n - 1$ and n , T_{mn}^{bu} is positive. This implies that a u -shell loses energy to all the b -shells but gains energy from the $(n - 1)^{\text{th}}$ and n^{th} b -shells. The quantity T_{mn}^{bu} is found to be small for $m < n$ in comparison with the transfer for $m > n$. Consequently, energy from a u -shell is mainly transferred to the b -shells at higher wave numbers. We had found earlier that the flux $\Pi_{b<}^{u>}(K)$ is much smaller in magnitude to the flux $\Pi_{b>}^{u<}(K)$. The fluxes and the transfer rates are consistent with each other. From Fig. 4 we also find that the energy transfer rate T_{1n}^{bu} from the n^{th} u -shell to the 1^{st} b -shell is positive, implying that the 1^{st} b -shell gains energy from the u -shells — this is a nonlocal transfer of energy from the large u -modes to the small b -modes. The flux $\Pi_u^{b<}$ observed in Section IV B (see Fig. 2) is due to this nonlocal transfer.

The homologous transfers are found to transfer energy from b -shells to u -shells (see Fig.4); this is in contrast to the net energy transfer and a majority of the non-homologous transfers which are from kinetic to magnetic. We find that the energy gained by a u -shell through the homologous transfers is larger than the *total* loss of energy by the u -shell through non-homologous transfers. Consequently, there is a *net* gain of energy by the u -shells in the inertial range. In Section IV B it was shown that the magnetic energy outside a b -sphere is lost to kinetic energy outside the u -sphere. It is now clear that this transfer arises primarily due to the homologous transfers from magnetic to kinetic.

The Fig. 4 shows energy transfer rates T_{mn}^{bu} , to b -shells from u -shells indexed as $n = 5, 6, 7, 8, 9$. In Fig. 5 we show the transfer rates T_{mn}^{bu} from the $n = 1$ u -shell to all the b -shells. Recall that the first u -shell comprises the small wave

number modes, $k = 1$ to 16. Comparing the magnitudes of T_{mn}^{bu} to the b -shells from the first u -shell (see Fig. 5) and from the u -shells at higher wavenumbers (see Fig. 4), we see that the energy transfer rate from the 1st u -shell dominates the transfers from all other u -shells. Hence, there is a large amount of *non-local* transfer from the first u -shell to the b -shells. In Section IV B we had claimed that there is no net kinetic energy transfer into any inertial range b -shell. Now we show this explicitly in Fig. 6 by plotting the net kinetic energy transferred into a b -shell ($=\sum_n T_{mn}^{bu}$) versus the shell index m (\diamond in the figure). From the figure, the net energy transferred into the inertial range b -shell can be seen to be nearly zero. We also plot in Fig. 6 the net kinetic energy transfer into a b -shell from all u -shells, *except* the first ($+$ in the figure). This quantity is now no longer zero and has a significant magnitude. Therefore, the non-local transfer from the first shell plays an important part in balancing the other kinetic energy transfers into an inertial range b -shell.

We have also computed the transfer rates of magnetic energy T_{mn}^{bb} from n^{th} to m^{th} b -shell. In Fig. 7 we have plotted the quantity T_{mn}^{bb} versus m for different values of n in the inertial range. We find that the differences in $T_{(n+\Delta n)n}^{bb}$ for any fixed $\Delta n (=n-m)$ are smaller than the standard deviation of their statistical fluctuations computed from the sampled data. Hence we can conclude that T_{mn}^{bb} is self-similar in the inertial range, dependent only on the difference Δn and independent of the location of the shell n . We find that the transfer rates T_{mn}^{bb} are negative for $m < n$ and they are positive for $m > n$ (see Fig. 7). Hence a b -shell gains energy from the b -shells of smaller wave numbers and loses energy to the b -shells of larger wave numbers. Since T_{mn}^{bb} is self-similar, the energy lost from a shell $(n-\Delta n)$ to n is equal to the energy lost from n to the shell $(n+\Delta n)$. Thus, the net magnetic energy transfer into any inertial range shell is zero, and the energy cascades from the smaller wave numbers to the higher wave numbers.

We now discuss the simulation results for the kinetic energy transfer rates T_{mn}^{uu} from the n^{th} to the m^{th} shell. The results are shown in Fig. 8 where we have plotted T_{mn}^{uu} versus m for various values of n . We find that the most dominant transfers are from the n^{th} u -shell to $m = n \pm 1$. From the sign of these transfers we see that kinetic energy is gained from $(n-1)^{\text{th}}$ shell and lost to $(n+1)^{\text{th}}$ shell. This means that the *local* transfers from the adjacent shells result in a *forward* cascade of energy towards the *large* wave numbers. The transfers from other shells are largely negligible except for the transfer to the shell $m = 1$ (shown boxed on the left of the figure), which represents a loss from high wave number modes to the $m = 1$ shell. This *non-local* transfer (to the first shell) produces an *inverse* cascade to the *small* wave numbers, observed earlier in Section IV B. Now it is clear that this inverse cascade is due to non-local transfers. The local and non-local transfers are seen to possess altogether different features: the former

is a forward cascade which seems largely self-similar, while the latter is an inverse cascade *only* to the first shell.

We schematically illustrate in Fig. 9 the energy transfer between shells. In this figure we show directions of the most significant transfers in the inertial range. The arrows indicate the directions of the transfers, and thickness of the arrows indicates the approximate relative magnitudes. Since the local transfer rates are self-similar, the transfers from any other shells in the inertial range will also show the same pattern. An inertial range b -shell gains significant amount of energy from the smaller u -shells through both local and non-local transfers, and it also locally gains energy from the smaller b -shells (T_{mn}^{bb}). The energy gained by a b -shell from the smaller b -shells is *exclusively* lost to the larger b -shells and the energy gained from the u -shells is mainly lost through homologous transfer (T_{nn}^{bu}) to the corresponding u -shell. A small fraction of the energy is also lost to the larger u -shells. In addition to the energy from the b -shells, a u -shell also gains energy from smaller u -shells by *local* transfer. The energy of u -shells is mainly lost locally to higher b -shells and u -shells, but a significant amount is also transferred to smaller u -modes (T_{mn}^{uu}) by a *non-local* inverse cascade.

As illustrated in Fig. 9, there is a transfer of energy from the first u -shell to the first b -shell. This is the most significant gain of magnetic energy from the kinetic energy. Under steady state the magnetic energy gained by the first shell gets transferred to the higher b -shells. This transfer yields the forward cascade of magnetic energy discussed in Section IV B

To summarise, we find that there are various types of energy transfers in MHD turbulence: local, nonlocal, homologous, and non-homologous. The main local transfers are the forward magnetic energy transfer and the forward kinetic energy transfer, the homologous transfer from the magnetic to the kinetic energy (all in the inertial range). There is nonlocal transfer from inertial range u -shells to the first b -shell and the first u -shell, and from the first u -shell to the b -shells. The most significant energy transfer is the transfer of kinetic energy from the first u -shell to magnetic energy in the first b -shell.

In this section we had extensively described various cascade rates (fluxes) and shell-to-shell energy transfer rates. It is clear that the complete picture is quite complex. In fact, some of the features we have seen contradicts earlier conjectures and results. These differences are discussed in the next section.

V. DISCUSSION

We have investigated the features of kinetic and magnetic energy transfer between scales at low values of cross-helicity in a quasi-steady state of forced 2-D MHD turbulence. Several interesting observations were made in our simulations. A summary of the results is given below. For the following discussion refer to Figs. 3 and 9.

- 1) There is a net transfer of energy from the kinetic to the magnetic.
- 2) There is an energy transfer to the large-scale magnetic field from the large-scale velocity field (u -sphere to b -sphere flux $\Pi_b^{u<}$ in Fig. 2), and also from the small-scale velocity field (flux from b -sphere to modes outside the u -sphere $\Pi_u^{b<}$ in Fig. 2). The former transfer is of a greater magnitude than the latter. The magnetic field enhancement is primarily caused by a transfer from the u -sphere to the b -sphere. Indeed the first few b -modes get most of this energy.
- 3) Other significant transfers, not noted in earlier work, are from the large-scale velocity field to the small-scale magnetic field (u -sphere to outside the b -sphere) and an interesting reverse transfer from the small-scale magnetic field to the small-scale velocity field (from modes outside the b -sphere to modes outside u -sphere).
- 4) There is an *inverse* cascade in the velocity field — this is consistent with the observation of Ishizawa and Hattori arising from numerical simulations [20] and is also consistent with the EDQNM closure calculations [6,7]. This inverse cascade of kinetic energy is driven by the reverse transfer of energy from magnetic to the velocity field at the small scales. Although the flux study points to an inverse cascade of kinetic energy, the shell-to-shell energy transfer rates reveal the following feature. There exists both an inverse and a forward transfer of kinetic energy. The inverse transfer is primarily *nonlocal*, coming from the larger wave numbers to the first few modes. The forward cascade is *local*, i.e., between same sized eddies and is self-similar in the inertial range.
- 5) There is a *forward* cascade of magnetic energy towards the small scales. This is consistent with other recent numerical simulations [20]. EDQNM closure calculations also yield a magnetic energy transfer to the small-scales [7]. The magnetic energy transfer is primarily *local* and is found to be self-similar in the inertial range.
- 6) In the inertial range we found a dichotomy between the homologous transfers (defined as the transfers between kinetic and magnetic energy shells of same wave numbers) and non-homologous transfers (which are the transfers between shells of different wave numbers). These transfers are more complex than had been anticipated [6] and are summarised and discussed in detail in Section IV C (also see Fig. 3).

The most important outcome of our study can be stated in the following points : (1) Enhancement of magnetic

energy occurs due to the energy transfer to the large-scale magnetic field from the large-scale velocity field, (2) there is a forward cascade of magnetic energy from the large-scale magnetic field to the small-scale magnetic field. Our results are important since they clarify some of the proposals made earlier regarding the physical mechanism for the generation of large-scale magnetic field. Pouquet [6] had found that the large-scale magnetic energy is destabilised by the small-scale magnetic energy. Ishizawa and Hattori [7] proposed that the large-scale magnetic energy is enhanced due to energy transfer from the small-scale velocity field to the large-scale magnetic field. Although we find such a transfer, the dominant transfer to the large-scale magnetic energy is from the large-scale kinetic energy. Pouquet and Patterson [27] proposed in context of 3-D turbulence that there an inverse cascade of energy from small-scale to large-scale magnetic field. However, our numerical calculations give a forward cascade in 2-D turbulence. A simulation should be done to verify whether this feature is also present in 3-D turbulence.

The EDQNM closure calculations yield a net transfer of energy to the large-scale magnetic field from the small-scales (magnetic+kinetic) [6,7]. In our simulations, the energy lost by the large-scale magnetic field to the small-scale magnetic field is much larger than the energy gained by the large-scale magnetic field from the small-scale velocity field. Hence, contrary to the predictions of EDQNM calculations, the large-scale magnetic field loses energy to the small-scales. A similar observation was also made by Ishizawa and Hattori in their simulations [20]. Thus, it appears that EDQNM calculations do not yield the correct strengths of the various transfers.

The picture obtained by us for the energy fluxes and the shell-to-shell energy transfers are consistent and complement each other. The fluxes and the transfer rates discussed here could find applications in the dynamo problem. In astrophysical objects, like galaxies and the sun, the magnetic field is thought to have arisen due to the amplification of a seed magnetic field. Our study has been performed over a quasi-steady state with a low Alfvén ratio. In order to understand the build-up of magnetic energy starting from a seed value it is important to perform a similar study at high Alfvén ratio. In some of the popular models, like the α -dynamo [38], the mean magnetic field gets amplified in presence of helical fluctuations. It must be borne in mind that our calculations are two-dimensional and devoid of magnetic helicity and kinetic helicity. A three-dimensional calculation (with the inclusion of magnetic and kinetic helicities) of various fluxes and shell-to-shell energy transfer rates will yield important insights on some unresolved issues concerning enhancement of magnetic energy.

The fluxes also find important applications in various phenomenological studies. For example, Verma *et al.* [39] estimated the turbulent dissipation rates in the solar wind and obtained the temperature variation of the solar wind

as a function of solar distance. The various cascade rates discussed here could be useful for various astrophysical studies. For example, $\Pi_{b<}^{u<}$ and $\Pi_{b>}^{u<}$ can be used for studying the variation of r_A of the solar wind.

The physics of MHD turbulence is still unclear. The studies of various fluxes and transfer rates shed light at various aspects which will help us in getting a better understanding of MHD turbulence.

ACKNOWLEDGMENTS

We thank Prof. R. K. Ghosh of Computer Science Dept., Indian Institute of Technology (IIT) Kanpur, for providing us computer time through the project TAPTEC/COMPUTER/504 sponsored by All India Council for Technical Education (AICTE).

- [1] G. Dar, M. K. Verma, and V. Eswaran, (submitted to Phys. Plasma)
- [2] M. Lesieur. *Turbulence in Fluids - Stochastic and Numerical Modelling*. Kluwer Academic Publishers, 1990.
- [3] R. H. Kraichnan. *Phys. Fluids*, 8:1385, 1965.
- [4] M. Dobrowolny, A. Mangeney, and P. Veltri. *Phys. Rev. Lett.*, 45:144, 1980.
- [5] Y. Zhou and W. H. Matthaeus. *J. Geophys. Res.*, 95:14881, 1990.
- [6] A. Pouquet. *J. Fluid Mech.*, 88:1, 1978.
- [7] A. Ishizawa and Y. Hattori. *chao-dyn/9810036*, 1998.
- [8] A. Pouquet, U. Frisch, and J. Leorat. *J. Fluid Mech.*, 77:321, 1976.
- [9] R. Grappin, U. Frisch, J. Leorat, and A. Pouquet. *Astron. Astrophys.*, 105:6, 1982.
- [10] R. Grappin, A. Pouquet, and J. Leorat. *Astron. Astrophys.*, 126:51, 1983.
- [11] S. J. Camargo and H. Tasso. *Phys. Fluids B*, 4:1199, 1992.
- [12] M. K. Verma and J. K. Bhattacharjee. *Europhys. Lett.*, 31:195, 1995.
- [13] M. K. Verma. *Phys. Plasma*, 6, 1999.

- [14] D. Fyfe and D. Montgomery. *J. Plasma Phys.*, 16:181, 1976.
- [15] A. Pouquet, P. L. Sulem, and M. Meneguzzi. *Phys. Fluids*, 31:2635, 1988.
- [16] H. Politano, A. Pouquet, and P. L. Sulem. *Phys. Fluids*, 1:2330, 1989.
- [17] D. Biskamp and H. Welter. *Phys. Fluids B*, 1:1964, 1989.
- [18] R. Kinney, J. C. McWilliams, and T. Tajima. *Phys. Plasma*, 2:3623, 1995.
- [19] M. K. Verma, D. A. Roberts, M. L. Golstein, S. Ghosh, and W. T. Stribling. *J. Geophys. Res.*, 101:21619, 1996.
- [20] A. Ishizawa and Y. Hattori. *J. Phys. Soc. Jpn.*, 67:441, 1998.
- [21] H. Politano, A. Pouquet, and V. Carbone. *Europhys. Lett.*, 43:516, 1998.
- [22] A. Basu, A. Sain, S. K. Dhar, and R. Pandit. *Phys. Rev. Lett.*, 81:2687, 1998.
- [23] W. Muller and D. Biskamp. physics/9906003, 1999.
- [24] M. K. Verma. *PhD thesis*. University of Maryland, 1994.
- [25] E. Marsch. In Reviews in Modern Astronomy, editor, *G. Klare*, volume 4, page 43. Heidelberg : Springer Verlag, 1990.
- [26] G. K. Batchelor. *Proc. Roy. Soc. (London)*, 2:413, 1950.
- [27] A. Pouquet and G. S. Patterson. *J. Fluid Mech.*, 85:395, 1978.
- [28] H. Tennekes and J. L. Lumley. *A first course in turbulence*. MIT press, 1972.
- [29] P. Frick and D. Sokoloff. *Phys. Rev. E*, 57:4155, 1998.
- [30] R.S.Miller, F.Mashayek, V.Adumitroaie, and P.Givi. *Phys. Fluids*, 3:3304, 1996.
- [31] M. Meneguzzi, U. Frisch, and A. Pouquet. *Phys. Rev. Lett.*, 47:1060, 1981.
- [32] J. Leorat, A. Pouquet, and U. Frisch. *J. Fluid Mech.*, 104:419, 1981.
- [33] Ya. B. Zeldovich. *Sov. Phys. JETP*, 4:460, 1957.
- [34] M. M. Stanisic. *The Mathematical Theory of Turbulence*. Springer-Verlag, 1985.
- [35] C. Canuto, M. Y. Hussaini, A. Quarteroni, and T. A. Zang. *Spectral Methods in Fluid Mechanics*. Springer-Verlag, New York, 1988.

- [36] J. A. Domaradzki and R. S. Rogallo. *Phys. Fluids A*, 2:413, 1990.
- [37] D. Biskamp and U. Bremer. *Phys. Rev. Lett.*, 72:3819, 1993.
- [38] M. K. Moffatt. *Magnetic field generation in electrically conducting fluids*. Cambridge University Press, 1978.
- [39] M. K. Verma, D. A. Roberts, and M. L. Golstein. *J. Geophys. Res.*, 100:19839, 1995.

FIGURE CAPTIONS

Fig. 1 Evolution of the total kinetic energy and the magnetic energy for simulations on grid sizes 512^2 and 128^2 . For 512^2 a quasi-steady magnetic energy is obtained over the period of the simulation. It is demonstrated in the 128^2 simulation that a quasi-steady magnetic energy eventually decays — a quasi-steady magnetic energy is obtained from $t = 60$ to 100.

Fig. 2 The simulation results of fluxes. The following fluxes have been plotted : the total flux (Π_{tot}), the kinetic energy flux from u -sphere to outside u -sphere $\Pi_{u>}^u$, the magnetic energy flux from b -sphere to outside b -sphere $\Pi_{b>}^b$, the energy flux from u -sphere to b -sphere $\Pi_{b<}^u$, the energy flux from u -sphere to modes outside the b -sphere $\Pi_{b>}^u$, the energy flux from b -sphere to modes outside the u -sphere $\Pi_{u>}^b$, the energy flux from modes outside u -sphere to modes outside the b -sphere $\Pi_{b>}^b$, and the net flux out of a b -sphere ($\Pi_{u>}^b + \Pi_{b>}^b$) have been plotted in this figure.

Fig. 3 The schematic illustration of the directions and the magnitudes of the fluxes plotted in Fig. V (also see Fig. 3.13 of Chapter 3). Also shown are the magnitudes of the kinetic energy input rate due to forcing, and the total dissipation of kinetic and magnetic energy. The fluxes are shown for $K = 20$ but are representative of the entire inertial range. All quantities have been time-averaged. The fluctuations of the fluxes (except $\Pi_{b<}^u$) and the dissipation rate are approximately equal to 0.005. The fluctuations in $\Pi_{b<}^u$ are higher and is approximately 0.01 .

Fig. 4 The energy transfer rate T_{mn}^{bu} from the n^{th} u -shell to the m^{th} b -shell. The loss of energy from the n^{th} u -shell to the m^{th} b -shell is defined to be positive.

Fig. 5 The energy transfer rate from the 1^{st} u -shell to the b -shells.

Fig. 6 The diamonds (\diamond) represent the net energy transfer into a b -shell from all the u -shells. The pluses (+) represent the net energy transfer into a b -shell from all u -shells except the 1st one.

Fig. 7 The energy transfer rate T_{mn}^{bb} from the n^{th} b -shell to the m^{th} b -shell. The loss of energy from the n^{th} b -shell to the m^{th} b -shell is defined to be positive.

Fig. 8 The energy transfer rate T_{mn}^{uu} from the n^{th} u -shell to the m^{th} u -shell. The loss of energy from the n^{th} u -shell to the m^{th} u -shell is defined to be positive. The boxed points represent energy transfer from the n^{th} u -shell to the 1st u -shell.

Fig. 9 A schematic representation of the direction and the magnitude of energy transfer between u -shells and b -shells. The relative magnitudes of the different transfers has been represented by the thickness of the arrows. The non-local transfers with the 1st shell have been shown by dashed lines.

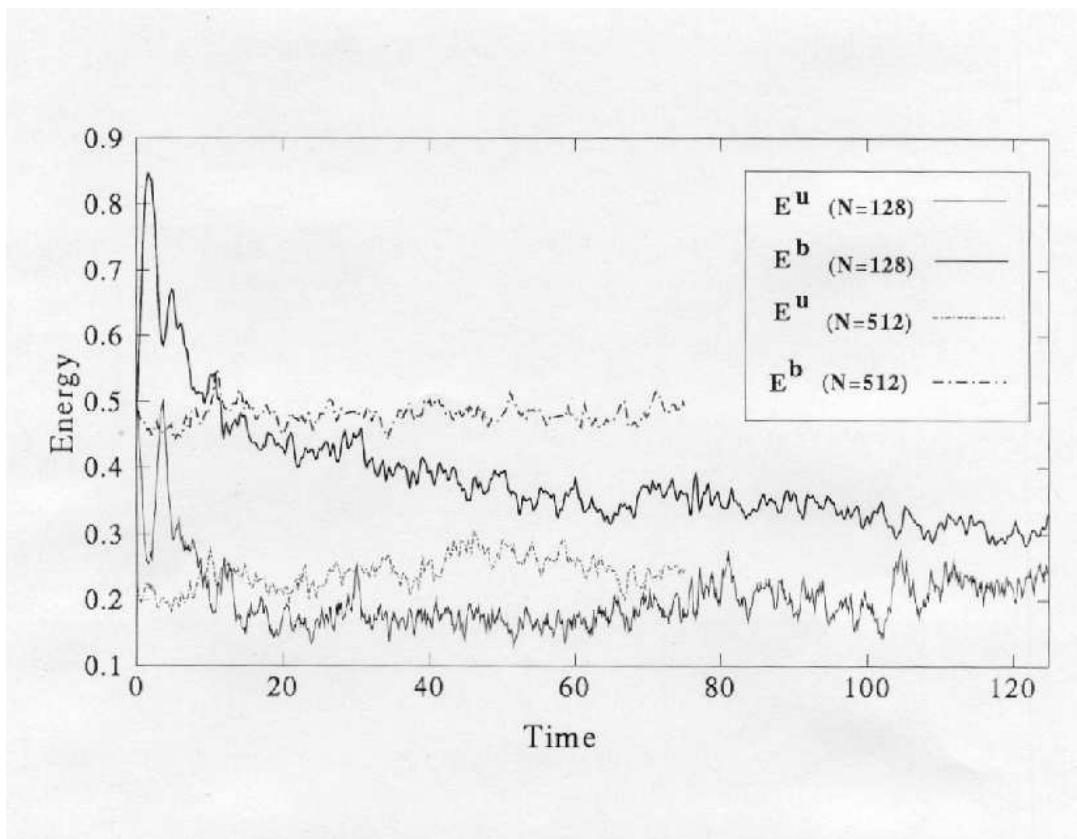


FIG. 1.

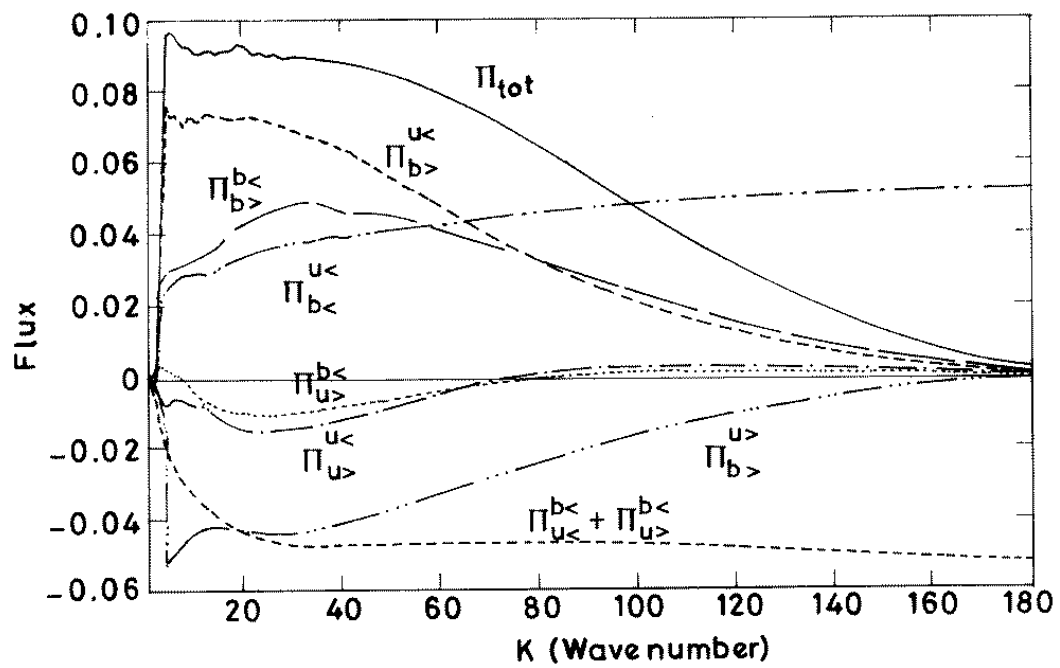


FIG. 2.

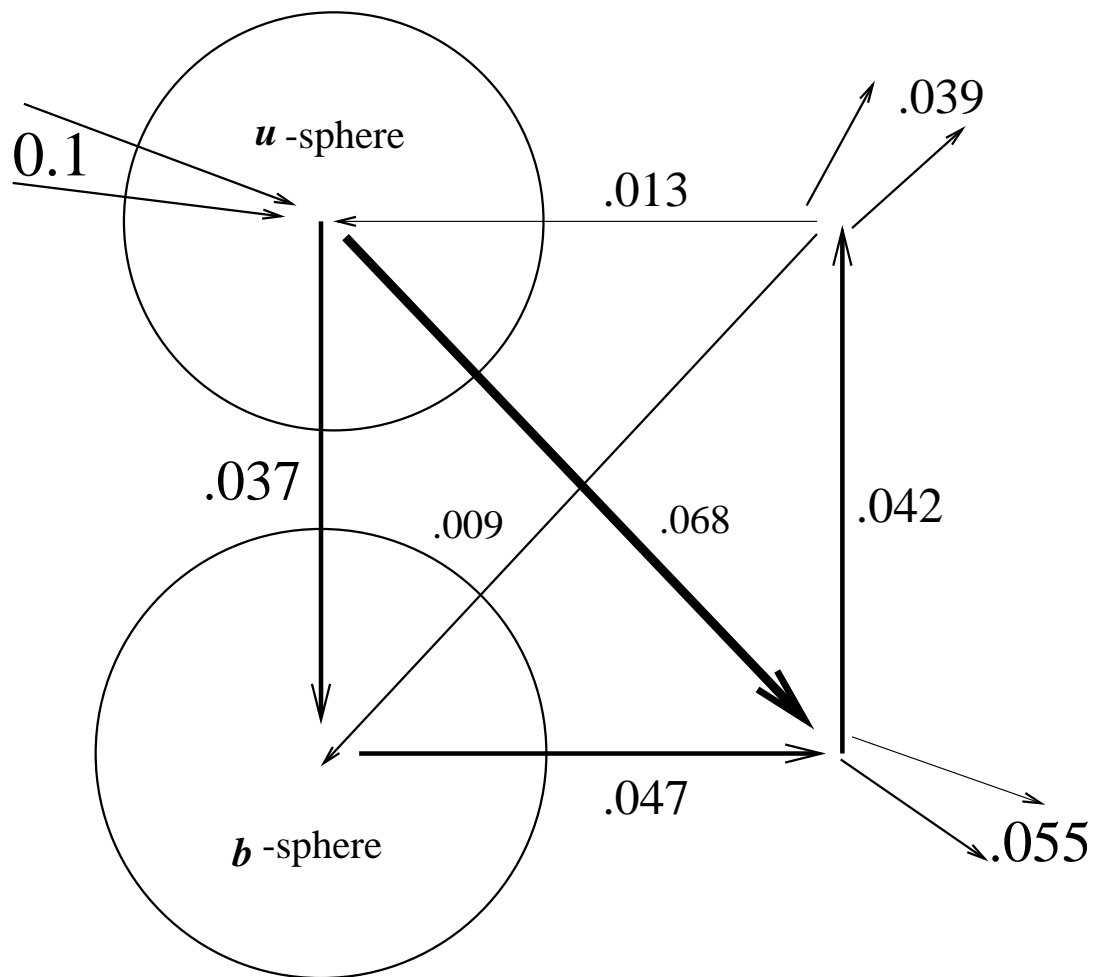


FIG. 3.

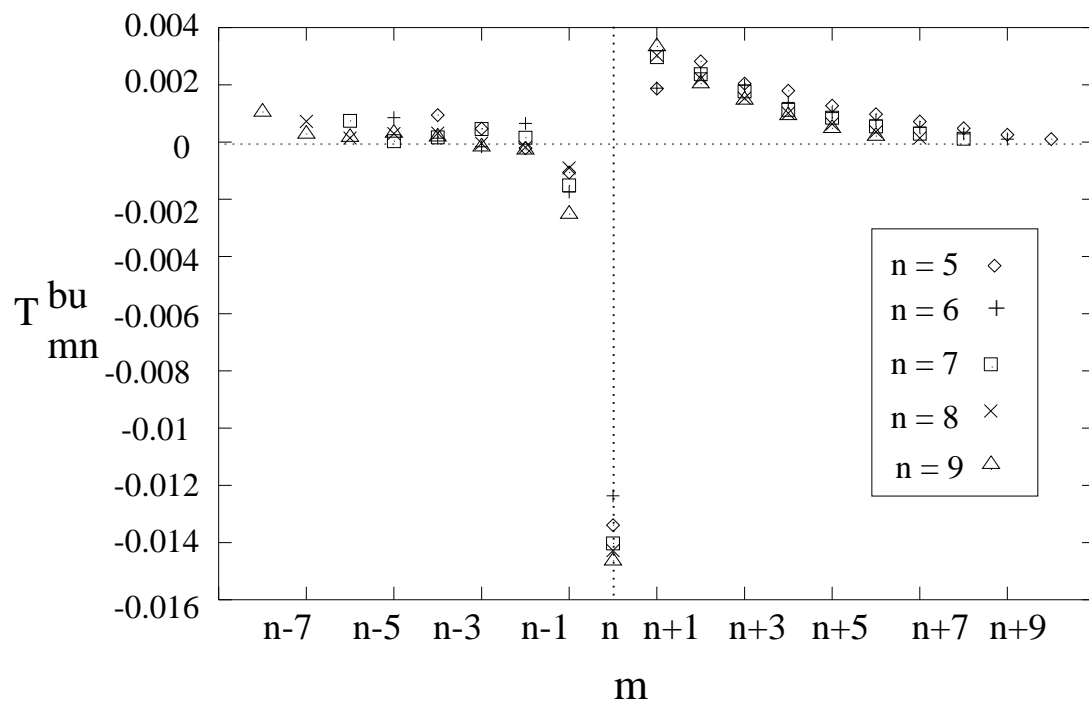


FIG. 4.

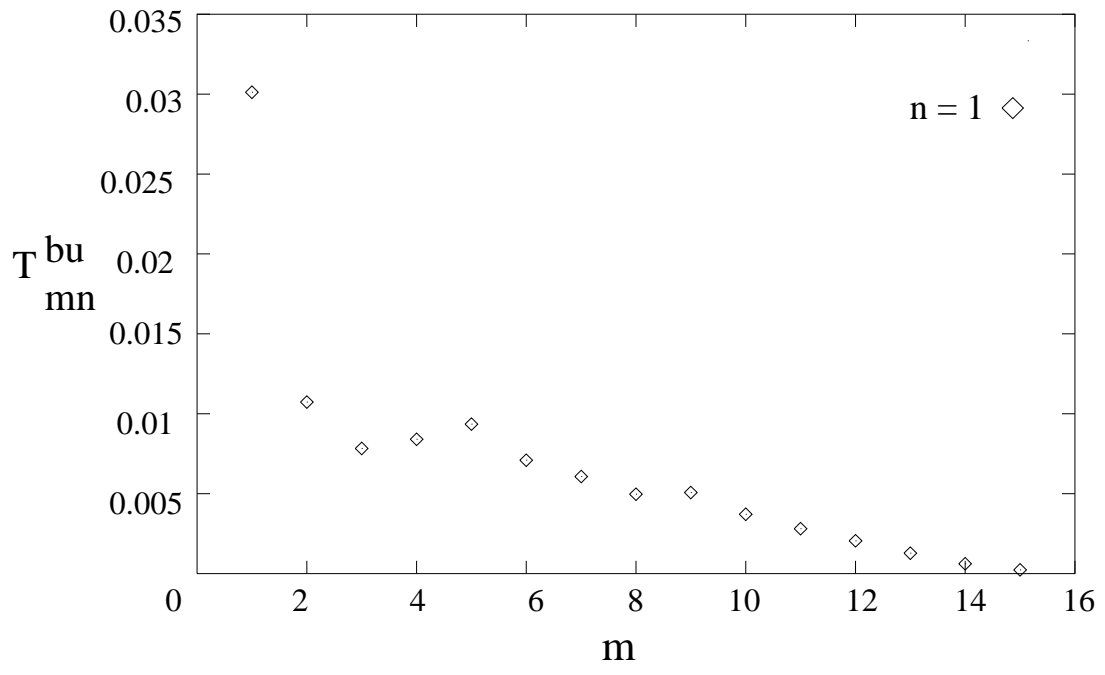


FIG. 5.

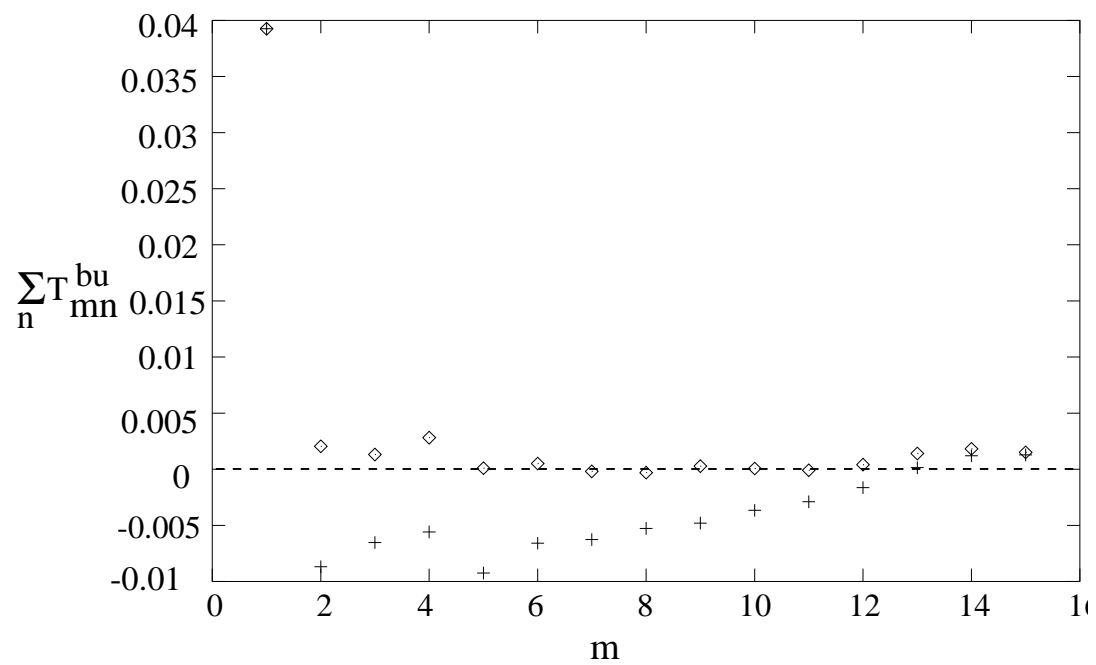


FIG. 6.

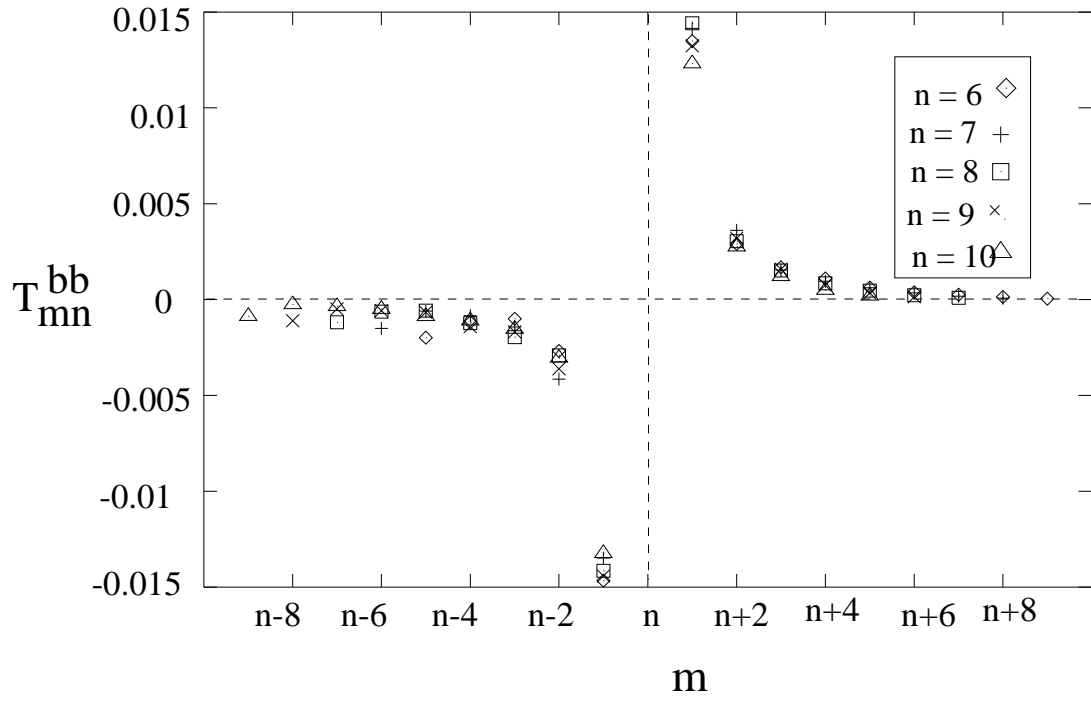


FIG. 7.

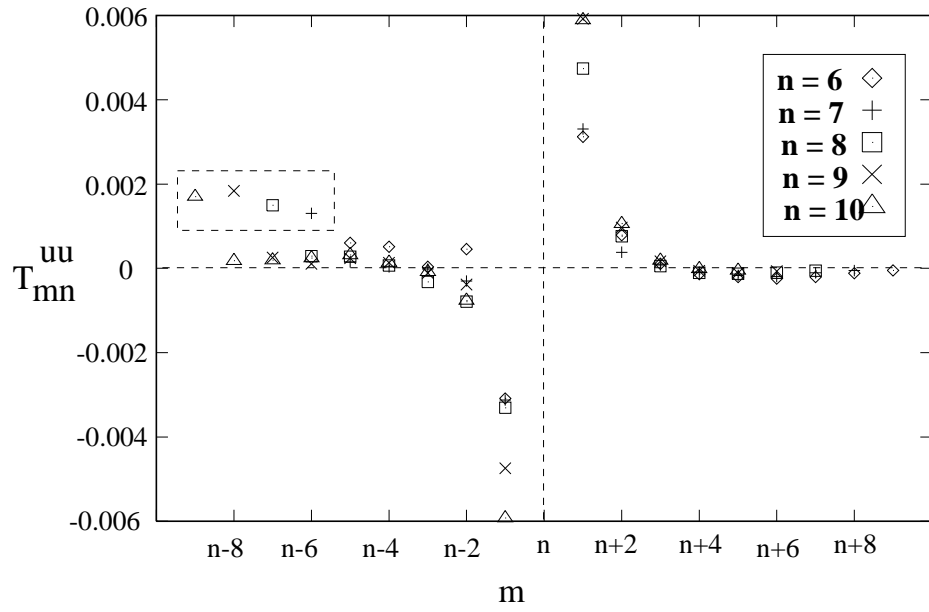


FIG. 8.

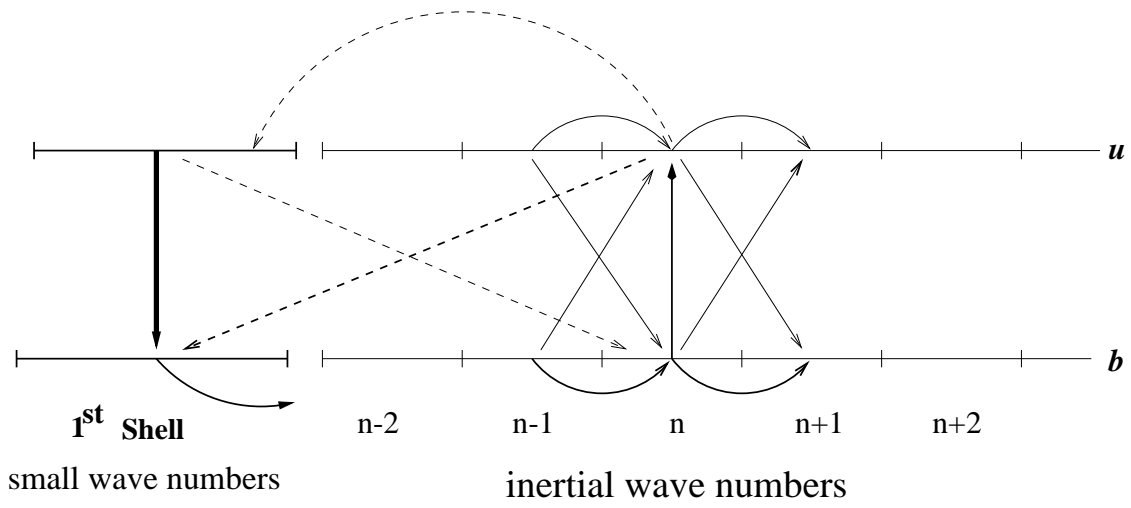


FIG. 9.